VLA detection of OH absorption from the elliptical galaxy NGC 1052

A. Omar[1], K. R. Anantharamaiah[1,*], M. Rupen[2], and J. Rigby[3]

[1] Raman Research Institute, C.V. Raman Avenue, Bangalore, 560 080, India
[2] National Radio Astronomy Observatory, Socorro, NM, USA
  e-mail: mrupen@aoc.nrao.edu
[3] Steward Observatory, University of Arizona, 933 N. Cherry Ave, Tucson, AZ 85721, USA
  e-mail: jrigby@as.arizona.edu

Abstract. VLA observations of OH absorption towards the elliptical galaxy NGC 1052 are presented. Both OH lines, at 1665 and 1667 MHz, were detected in absorption towards the center of NGC 1052. The hyperfine ratio of the two OH lines (τ_{1667}/τ_{1665}) is 2.6 ± 0.8 as compared to 1.8 expected for the excitation under LTE conditions for an optically thin cloud. The column density of OH is estimated to be $2.73\,(\pm 0.26) \times 10^{14}$ cm^{-2} assuming $T_{\rm ex} \sim 10$ K. The centers of both the OH lines are redshifted from the systemic velocity of the galaxy by ~ 173 km s^{-1}. The velocity of OH line coincides with the velocity corresponding to the strongest HI absorption. We suggest that OH absorption is arising from a molecular cloud falling towards the nucleus. The OH line, though narrower, is found to be within the much broader and smoother H_2O megamaser emission. The possible link between OH/HI and H_2O emission is discussed.

Key words. galaxies: active – galaxies: individual: NGC 1052 – galaxies: ISM – radio lines: galaxies

1. Introduction

The most extensive and conclusive confirmation for the presence of cold interstellar material in early-type galaxies came from observations of dust with the Infrared Astronomical Satellite (IRAS) (Neugebauer 1984; Knapp et al. 1985; Knapp et al. 1989). Sensitive observations of HI (van Gorkom et al. 1989; Huchtmeier et al. 1995) have also shown that elliptical galaxies contain a significant amount of cold interstellar matter. The molecular contents of elliptical galaxies has been studied mainly through CO observations of infrared bright elliptical galaxies (Wang et al. 1992; Wiklind et al. 1995; Knapp & Rupen 1996). These observations resulted in the detection of molecular gas in several galaxies in emission and four galaxies in absorption, indicating that the overall detection rate of CO in elliptical galaxies is about 10–15%. The OH radical in absorption is also a good tracer of molecular gas in interstellar clouds (Liszt & Lucas 1996). Single dish OH surveys (Schmelz et al. 1986; Baan et al. 1992; Staveley-Smith et al. 1992; Darling & Giovanelli 2000) of several hundred galaxies of various types resulted in the detection of about 3 dozen galaxies, of which none was an elliptical.

NGC 1052, a moderately luminous ($L_{\rm b} = 1.6 \times 10^{10}\ L_\odot$) elliptical galaxy of type E4, is a member of a small group in the Cetus–I cloud. There are several estimates of the velocity for this system in the literature, which differ from each other by a few tens of km s^{-1}. We adopt $V_{\rm hel} = 1474 \pm 10$ km s^{-1}, estimated from the optical emission lines (de Vaucouleurs 1991), which implies that NGC 1052 is at a distance of 21 Mpc (assuming $H_0 = 70$ km s^{-1} Mpc^{-1} and $q_0 = 0$). It is classified as a LINER (Fosbury et al. 1978; Ho et al. 1997) and is known for its several water megamasers (Braatz et al. 1996; Claussen et al. 1998). HI absorptions, redshifted from the systemic velocity, were detected at 1486, 1523 and 1646 km s^{-1} against the nuclear continuum source (van Gorkom et al. 1986). NGC 1052 was reported to have CO emission as well as absorption by Wang et al. (1992), but later observations by Wiklind et al. (1995) failed to confirm those detections. More recently, Knapp & Rupen (1996) have reported a possible CO absorption from NGC 1052 near 1622 km s^{-1}. Since the reported CO detections are quite noisy, it remains uncertain whether NGC 1052 has a molecular component associated with the HI (21 cm) absorption.

Here we report the first detection of 1665 and 1667 MHz OH absorption in NGC 1052. The next section describes the observational details and results. Subsequent sections compare these results with observations at

Table 1. Observation parameters.

Parameter	Value
Date of observation	1998 Sep. 03
RA, Dec (J2000.0)	02 41 04.79, –08 15 20.75
Observing duration (hrs)	5
Range of baselines (km)	0.1–11 (B config)
Observing frequencies (MHz)(IF1,IF2)	1656.50, 1658.30
Bandwidth per IF (MHz)	1.562
Number of spectral channels	64
Polarizations	RCP & LCP
Synthesised beam (Natural Weight)	$6.4'' \times 4.3''$, PA = $9.7°$
Velocity resolution	4.4 km s^{-1}
Frequency resolution (kHz/channel)	24.4
Amplitude calibrator	0137+331 (3C 48)
Phase calibrator	0240–231
Bandpass calibrator	0319+415 (3C 84)
rms noise per channel (mJy beam^{-1})	0.7

optical, X-ray, and other wave bands, and discuss some of the implications.

2. Observations and results

NGC 1052 was observed in the B configuration of the VLA, which has interferometric baselines ranging from 100 m to 11 km. Data were recorded in the 4IF correlator mode, recording 1.5625 MHz in each of the two circular polarizations for two frequency bands, one centered at 1656.5 and other at 1658.3 MHz. The details of the observations are listed in Table 1. The data were reduced in AIPS using standard calibration and imaging methods. The amplitude, phase and frequency response of the antennas were calibrated separately for each IF. The phase and amplitude gains of the antennas were derived from observations of the standard VLA calibrator 0240–231 at intervals of 30 min. The flux scale was set using Baars et al. (1977) flux density of the standard VLA calibrator 3C 48. A combined bandpass spectrum was generated using all the data taken on the amplitude and phase calibrators as well as on the strong radio source 0319+415 (3C 84). A continuum data set was formed by averaging the calibrated visibility data of 50 line-free channels. The continuum data set was self-calibrated and the resulting antenna gain corrections were applied to every spectral channel separately. The continuum emission common to all channels was removed using the task "UVLIN" inside AIPS. Continuum–free images for all channels were made and the source region was searched for absorption. Both 1665 and 1667 MHz lines were detected, in each of the two circular polarizations. Although, a part of the band centered at 1656.5 MHz was affected by interference, the detected 1665 MHz line was outside the affected region.

The core/jet morphology in the continuum image of NGC 1052 is in accordance with the previous observations by Jones et al. (1984). The peak continuum flux density of the core is ~1.14 Jy. The total flux density including contributions from the two radio lobes is ~1.23 Jy. The continuum image (Fig. 1) shows that the radio axis is at a position angle (E to N) of 103°. The two radio lobes are

asymmetrically located about the radio nucleus, being $14''$ to the east and $8''$ to the west. The continuum nucleus and the line absorption are unresolved with the synthesised beam ($6.4'' \times 4.3''$, PA = $9.7°$). Both 1665 and 1667 MHz lines are detected at a redshifted velocity of ~173 km s^{-1} with respect to the systemic velocity of the galaxy. The column density of OH can be estimated from

$$N_{\text{OH}} = 2.35 \times 10^{14} \, T_{\text{ex}} \int \tau_{1667} \, \mathrm{d}V \text{ cm}^{-2} \qquad (1)$$

(Dickey et al. 1981; Liszt & Lucas 1996) where T_{ex} is the excitation temperature in Kelvins, τ_{1667} is the optical depth of the 1667 MHz line and V is the velocity in km s^{-1}; for NGC 1052, above equation gives an OH column density of $2.73 \, (\pm 0.26) \times 10^{14} \, (T_{\text{ex}}/10) \text{ cm}^{-2}$ towards the center. For the two lobes, we estimate an average 3σ upper limit of OH absorption as ~0.10. This upper limit implies that 0.6% absorption seen towards the nucleus is undetectable from either of the lobes even if absorbing gas covers the entire continuum source.

The AIPS gaussian fitting routine "SLFIT" was used to derive the line parameters. The peak optical depth of the 1667 MHz line is $5.8 \, (\pm 0.2) \times 10^{-3}$ and that of the 1665 MHz line is $2.9 \, (\pm 0.1) \times 10^{-3}$. The *FWHM* of 1667 and 1665 MHz lines are 18.8 ± 1.3 and 14.5 ± 2.6 km s^{-1} respectively. Given the uncertainity in the overall shape of the 1665 MHz line due to low optical depth, profiles of the 1665 and 1667 MHz lines can be considered similar. The ratio of the integrated optical depth is 2.6 ± 0.8 which is marginally higher than that expected (viz. 1–1.8) for excitation in thermal equillibrium. The mean value of 1667 to 1665 MHz line ratio is about 1.6 for galactic diffuse clouds (Dickey et al. 1981).

3. Discussion

3.1. Link with HI and X-ray absorbing column

HI components in NGC 1052 have been seen in absorption at 1486, 1523 and 1646 km s^{-1}, which are redshifted from the systemic velocity (van Gorkom et al. 1986). The $N(\text{HI})/T_{\text{ex}}$ values of three components are 0.6×10^{18}, 1.0×10^{18} and 1.4×10^{18} cm^{-2} respectively. The strongest absorption ($\tau \sim 0.02$) is at 1646 km s^{-1} with a *FWHM* of about 35 km s^{-1}. Due to the similarity in the velocity of OH absorption with the highest redshifted component of HI absorption, it is reasonable to associate this HI component with the OH detected in these observations. It is interesting that the velocity of OH absorption matches very well with the strongest HI absorption component at 1646 km s^{-1} even after a difference of about 16 years in the observations. The stability of OH/HI line suggests that the absorbing cloud covers a substantial fraction of the milliarcsec VLBI core in which most of the radio emission lies (Jones et al. 1984; Kameno et al. 2001). The integrated optical depth ratio of HI to OH is ~6, which is in accordance with the values obtained for the galactic diffuse clouds (Dickey et al. 1981). The linewidth ratio of HI
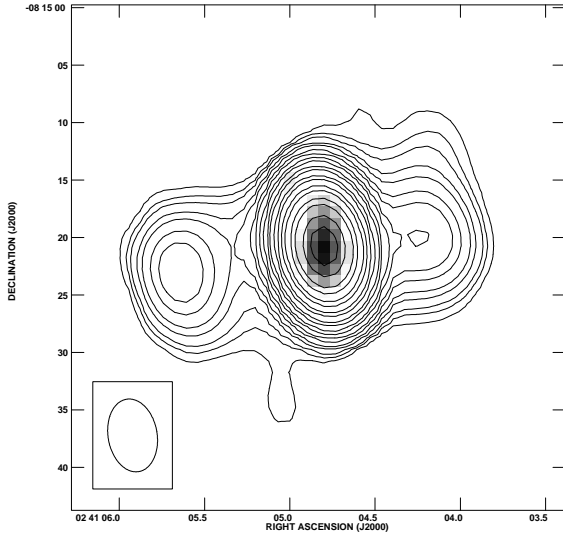
Fig. 1. The radio continuum image of NGC 1052 drawn as contours with levels of 1.8 mJy beam^{-1} × (1, 1.5, 2, 3, 4, 6, 8, 12, 16, 24, 32, 48, 64, 96, 128, 192, 256, 384, 512). The peak flux density in the contour image is 1.14 Jy beam^{-1}. The peak flux densities of the E and W lobes are 22.3 and 19.4 mJy beam^{-1} respectively. The grey scale represents the velocity–integrated optical depth of the 1667 MHz OH absorption. The synthesised beam depicted in the bottom left corner is $6.4'' \times 4.3''$, PA = 9.7°.
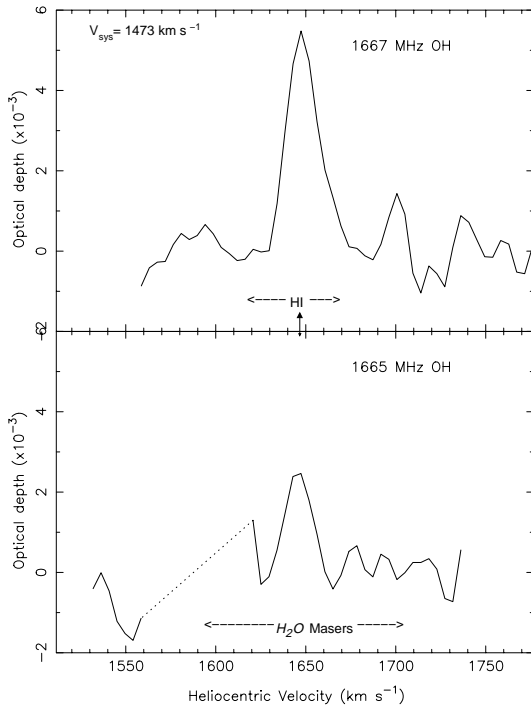
Fig. 2. A plot of the optical depth of 1667 and 1665 MHz absorption lines towards the nucleus of NGC 1052. The spectrum has been Hanning smoothed offline using a window of 3 adjacent channels. The figure displays the entire velocity coverage by VLA observations. The region marked by dashed lines in 1665 MHz spectrum was affected by interference. The velocity range over which HI absorption and H$_2$O masers are observed are indicated in the top and bottom frames respectively. The systemic velocity is indicated on top left corner of the upper frame.

to OH is ∼2, which suggests that the excitation of OH is restricted to some preferred regions inside the cloud. If redshifted absorption is considered as an evidence of infall of gas to the nucleus, where a small fraction of the gaseous mass is converted to luminosity, then, the association of a large amount of molecular gas with the neutral gas will imply a lower efficiency of the central engine in converting mass to luminosity. The observed line widths (*FWHM*) viz. ∼18 km s^{-1} of the two OH absorption is considerably higher than would be expected (∼1 km s^{-1}) from purely thermal motions, assuming the gas temperature is at most a few tens of K. However, if the gas is very close (within few pc) to the nucleus, some kinematical effects will tend to broaden the observed absorption line e.g., turbulence may set up to overcome the gravitational collapse against the nucleus. If the gas is in a disk, then, a velocity gradient along the disk, as seen in some megamaser galaxies (e.g. Hagiwara et al. 2000), can explain the observed line width of the OH absorption. On the other hand, if the observed dispersion is considered due to conglomerate of individual clouds in virial equilibrium, a binding mass will be about 10^6 $M_\odot$, a value close to that seen in some giant molecular clouds (GMCs) of our galaxy. The typical velocity width of such GMCs has been estimated close to 10 km s^{-1} (Stark & Blitz 1978).

The gas is expected to be much hotter in the vicinity of an AGN due to enhanced Lyα pumping which in turn will increase the T_{ex} to a few thousand kelvin. Assuming, $T_{ex} \sim 1000$ K, the predicted total N(HI) will be 2.0×10^{21} cm^{-2} including all three HI components. For the detected OH component, taking the relative abundance ratio of OH/H$_2 = 1 \times 10^{-7}$ (Guèlin 1985; Liszt & Lucas 1999), the implied column density of H$_2$ is 2.73×10^{21} $(T_{ex}/10)$ cm^{-2}. The implied CO column density is about 5.5×10^{14} cm^{-2}, which is about 10 times higher than predicted from CO observations. In comparison, X-ray observations indicate a hydrogen column density greater than 1×10^{23} cm^{-2} (Weaver et al. 1999), which is significantly higher than the total hydrogen column estimated via radio observations (HI & OH). This excess column density inferred from X-ray data has been seen in many active galaxies, and, was explained due to excess absorption by a combination of dust and partially ionized gas (Gallimore et al. 1999). It should be noted here that since HI and OH absorptions are spatially unresolved, the estimated values of OH and HI column densities are only a lower limit. Also, X-ray absorption is arising towards the nucleus which is free-free absorbed at wavelengths corresponding to the HI and OH absorptions (Kameno et al. 2001), therefore, radio observations are sampling off nuclear gas which may be of different composition than the gas probed via X-ray observations.

3.2. Link with H$_2$O megamasers?

It is very surprising that the OH absorption, though narrower than the water maser emission, is coincident

with the velocity centroid of the 22 GHz H_2O masers. NGC 1052 is the only known elliptical galaxy having H_2O megamaser emission. The megamasers and their link with AGNs are generally understood in terms of obscuring torus models. The link is thought to be a consequence of irradiation of the inner face of the torus by hard X-rays from the nuclear continuum source, which enhances the water abundance within a molecular layer at a temperature of 400–1000 K (Neufeld et al. 1994). H_2O megamasers of NGC 1052 are unusual in showing a relatively smooth profile which moves in velocity over time by about 70 km s^{-1} on a time scale of a year (Braatz et al. 1996). Water masers in NGC 1052 are distributed along the jet rather than perpendicular to it (Claussen et al. 1998) unlike in NGC 4258 in which water masers are originating in a torus (see Miyoshi et al. 1995). Claussen et al. (1998) suggested that these masers are excited by shocks in to circumnuclear molecular cloud, or alternatively, amplifying radio continuum emission of the jet by foreground molecular clouds. It should be noted that the shocks can also enhance the abundance of OH by dissociation of H_2O before the gas is cooled down below 50 K (Wardle 1999), however, the observed column density of OH is one order of magnitude less than that predicted. A drift in the velocity of maser feature was considered as a consequence of the moving jet which will illuminate different parts of the foreground H_2O masing cloud. Efficient maser emission will take place at total column density (N_H) below the quenching density which is estimated as $10^{25}-10^{27}$ cm^{-2} for NGC 1052 (see Weaver et al. 1999). This upper limit on column density is well above than that predicted from our observations. However, it is not clear how HI/OH are quite stable over a long period of time while H_2O emission changes substantially over a short time scale. Further simultaneous observations of HI, OH and H_2O masers are required to make a connection between molecular gas traced by OH absorption and H_2O masing gas.

4. Summary

These VLA observations have resulted in the first detection of OH absorption in an elliptical galaxy. Both, 1665 and 1667 MHz OH absorption, were detected from the elliptical galaxy NGC 1052. The linewidths of both the OH lines are significantly large as compared to that expected for a cloud in thermal conditions at few tens of K. The gas is predicted to be close to the nucleus. A remarkable coincidence of velocity is found with the strongest and redshifted HI absorption and H_2O emission, however link to the megamaser emission is still not understood. Based on the abundance ratio of OH/H_2 as 1×10^{-7}, it is predicted that the column density of molecular gas in NGC 1052 is comparable to HI. Higher angular and spectral resolution observations would be usefull for detail kinematics of the OH absorption while simultaneous observations of H_2O and HI/OH observations would be neccessary to understand the link between masing gas and molecular gas traced by OH absorption.

References

Baan, W. A., Haschick, A. D., & Henkel, C. 1992, AJ, 103, 728
Baars, J. W. M., Genzel, R., Pauliny-Toth, I. I. K., & Witzel, A. 1977, A&A, 61, 99
Braatz, J. A., Wilson, A. S., & Henkel, C. 1996, ApJ, 106, 51
Claussen, M. J., Diamond, P. J., Braatz, J. A., Wilson, A. S., & Henkel, C. 1998, ApJ, 500, L129
Darling, J., & Giovanelli, R. 2000, AJ, 119, 3003
de Vaucouleurs, G., de Vaucouleurs, A., Corwin, H. G. Jr., et al. 1995, in Third Reference Catalogue of bright galaxies, version 3.9
Dickey, J. M., Crovisier, J., & Kazès, I. 1981, A&A, 98, 271
Fosbury, R. A. E., Mebold, U., Goss, W. M., & Dopita, M. A. 1978, MNRAS, 183, 549
Gallimore, J. F., Baum, S. A., O'Dea, C. P., Pedlar, A., & Brinks, E. 1999, ApJ, 524, 684
Guèlin, M. 1985, in Molecular Astrophysics, ed. by W. F. Diercksen, W. F. Huebner, & P. W. Langhoff (Reidel), 23
Hagiwara, Y., Diamond, P. J., Nakai, N., & Kawabe 2000, A&A, 360, 49
Ho, L. C., Filippenko, A. V., & Sargent, W. L. W. 1997, ApJS, 112, 315
Huchtmeier, W. K., Sage, L. J., & Henkel, C. 1995, A&A, 300, 675
Jones, D. L., Wrobel, J. M., & Shaffer, D. B. 1984, ApJ, 276, 480
Kameno, S., Sawada-Satoh, S., Inoue, M., Zhi-Qiang, S., & Kiyoaki, W. 2001, PASJ, 53, 169
Kazes, L., & Dickey, J. M. 1985, A&A, 152, 9
Knapp, G. R., Guhathakurta, P., & Kim, D. W. 1989, ApJS, 70, 329
Knapp, G. R., & Rupen, M. P. 1996, ApJ, 460, 271
Knapp, G. R., Turner, E. L., & Cunniffe, P. E. 1985, AJ, 90, 454
Liszt, H., & Lucas, R. 1996, A&A, 314, 917
Liszt, H., & Lucas, R. 1999, Highly Redshift Radio Lines, ed. by Carilli et al., ASP Conf. Ser., 156, 188
Miyoshi, M., Moran, M., Herrnstein, J., et al. 1995, Nature, 373, 127
Neufeld, D. A., Maloney, P. R., & Conger, S. 1994, ApJ, 436, L127
Neugebauer, G. 1984, ApJ, 278, L1
Schmelz, J. T., Baan, W. A., Haschick, A. D., & Eder, J. 1986, AJ, 92, 1291
Stark, A. A., & Blitz, L. 1978, ApJ, 225, L15
Staveley-Smith, L., Norris, R. P., Chapman, J. M., et al. 1992, MNRAS, 258, 725
van Gorkom, J. H., Knapp, J. H., Ekers, S. M., et al. 1989, AJ, 97, 708
van Gorkom, J. H., Knapp, G. R., Raimond, E., Faber, S. M., & Gallagher, J. S. 1986, AJ, 91, 791
Wang, Z., Kenney, J. D. P., & Ishizuki, S. 1992, AJ, 104, 2097
Wardle, M. 1999, ApJ, 525, L101
Weaver, K. A., Wilson, A. S., Henkel, C., & Braatz, J. A. 1999, ApJ, 520, 130
Wiklind, T., Combes, F., & Henkel, C. 1995, A&A, 297, 643